

# Performance enhancement of a joint transform correlator using the directionality of a spatial light modulator

Mei-Li Hsieh\*

Eung-Gi Paek, FELLOW SPIE

Charles L. Wilson

National Institute of Standards and  
Technology  
Gaithersburg, Maryland 20899

Ken Y. Hsu, MEMBER SPIE

National Chiao Tung University  
Institute of Electro-Optical Engineering  
Hsin-Chu, Taiwan

**Abstract.** We observe that conventional electrically addressable spatial light modulators have different transfer functions along the fast (horizontal) and the slow (vertical) directions. We then propose to use the directionality of a spatial light modulator to increase the performance of a joint transform correlator. Our experimental results show that input space-bandwidth product of a joint transform correlator can be significantly increased by recording a hologram so that interference fringes run along the fast (horizontal) direction of a spatial light modulator. © 1999 Society of Photo-Optical Instrumentation Engineers. [S0091-3286(99)00412-2]

Subject terms: optical pattern recognition; spatial light modulators; optical information processing; joint transform correlator; optical security.

Paper 980467 received Dec. 16, 1998; revised manuscript received May 24, 1999; accepted for publication May 24, 1999.

## 1 Introduction

Optical pattern recognition is gaining increased attention and shows great promise due to the recent developments in device technologies including high speed spatial light modulators (SLMs) and detectors and a new demand from internets and biometrics. The joint transform correlator<sup>1</sup> has some clear advantages over VanderLugt-type correlators<sup>2</sup> because it does not require critical filter positioning, and real-time operation (both as an input and as a filter) is easier using<sup>3,4</sup> commercially available low-cost SLMs. However, one of the main factors that have hampered practical uses of a joint transform correlator is the lack of available SLMs that have high enough resolution to record interference fringes formed by an input pattern and a reference pattern. Although the grating period of an interference fringe can be increased by simply increasing the focal length of a Fourier lens, this can result in a bulky correlator and so is not desirable. Also, although optically addressable SLMs with high resolution are available,<sup>5</sup> electrically addressable SLMs are still widely used in optical pattern recognition due to their easier operation and lower cost.

Recently, we observed that the resolution of an electrically addressable SLM is significantly different along the horizontal (fast scan) and the vertical (slow scan) directions. In this paper, we utilize the directionality of an electrically addressable SLM to improve the performance of a joint transform correlator in terms of input space-bandwidth product and efficiency.

## 2 Directional Dependence of the Resolution (or Transfer Function) of an Electrically Addressable LC-SLM

Figure 1 illustrates the directional dependence of the resolution of an electrically addressable SLM. The structure and the addressing scheme of an LC-SLM are shown in Fig. 1(a). A serial signal containing one horizontal line is transferred through a shift register along the fast scan (horizontal) direction and is latched when the whole line is in place. The latched line signal is loaded onto the  $j$ 'th vertical line, which is designated by the vertical addressing signal. In this way, an image pattern is loaded line by line from top to bottom along the slow scan (vertical) direction.

The phenomena of the directional dependence of the resolution of an SLM is sketched in Figs. 1(b) and 1(c). A vertical grating shown in Fig. 1(b) is blurred along the fast scan (horizontal) direction. Such a blur along the fast scan direction is attributed to the limited response time of the driver electronics and the liquid crystal. On the other hand, a horizontal grating in Fig. 1(c) has clear boundaries because the addressing is achieved at a much slower rate along the vertical direction and the blur occurring along the fast scan direction does not affect the grating.

## 3 Experimental Results to Characterize the Directional Dependence of Resolution

Three different types of liquid crystal (LC) SLMs are used for this experiment.<sup>†</sup> These are denoted as type I, II and III

\*Permanent address: National Chiao Tung University, Institute of Electro-Optical Engineering, Hsin-Chu, Taiwan.

<sup>†</sup>Certain commercial equipment or components are identified in this paper only to specify the experimental procedure adequately. Use of this equipment or components does not constitute an endorsement by the National Institute of Standards and Technology (NIST) or any other agency of the Department of Commerce.

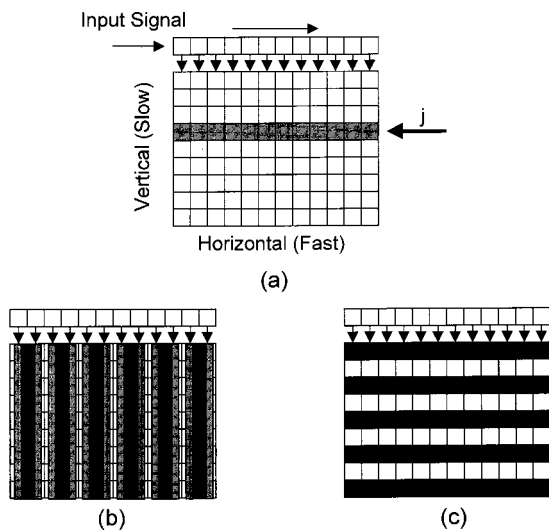


**Fig. 1** (a) Structure and addressing scheme of an electrically addressable SLM, (b) an SLM image of a vertical grating (the image is smeared along the fast scan direction), and (c) an SLM image of a horizontal grating (no smearing).

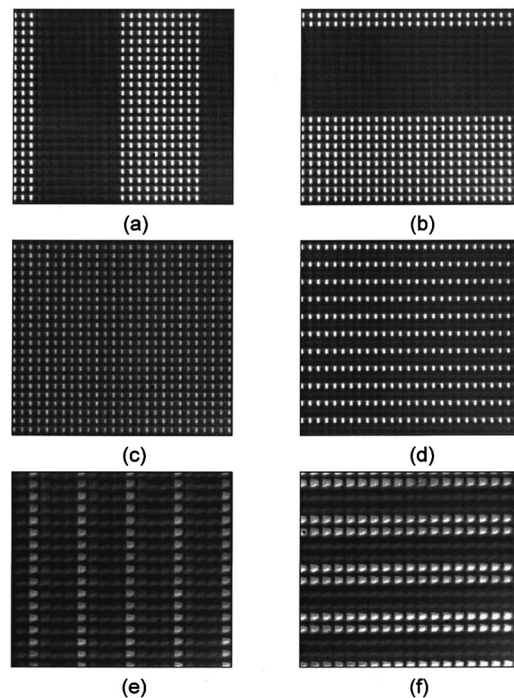
SLMs. Type I and II SLMs were manufactured by the same company and type III was by a different company. The type I SLM has  $640 \times 480$  pixels within a display area of  $15.36 \times 11.52$  mm, and each pixel has an aspect ratio of 1:1 ( $24 \times 24 \mu\text{m}$ ). The type II SLM has  $320 \times 240$  pixels with an active display area of  $4.8 \times 3.6$  mm and a pixel pitch size of  $15 \times 15 \mu\text{m}$ . The type III SLM has  $800 \times 600$  pixels, and each switchable area is  $26 \times 24 \mu\text{m}$ .

Figure 2 shows the experimental microscopic images of grating patterns with different periods and orientations. Figures 2(a) to 2(d) were obtained using type I SLMs and similar results were obtained for type II SLMs also. Figures 2(e) and 2(f) were obtained with a type III SLM. The grating periods of Figs. 2(a) and 2(b) are the same and are 20 pixels, but the gratings are oriented along the vertical and the horizontal directions in Figs. 2(a) and 2(b), respectively. In the case of these large-period gratings, both image patterns are displayed faithfully regardless of orientation.

However, when the grating period is small (2 pixels), as in Figs. 2(c) and 2(d), the shape of the vertical grating [Fig. 2(c)] is significantly smeared along the fast scan direction and so the grating pattern is not easily recognizable. On the other hand, the horizontal gratings shown in Fig. 2(d) has a clear pattern with high contrast.

Figures 2(e) and 2(f) are grating patterns obtained for a type III SLM with a grating period of 4 pixels. As expected, the vertical grating [Fig. 2(e)] is smeared along the fast scan direction, while the horizontal grating [Fig. 2(f)] is sharply defined.

To confirm reproducibility of the results, we tested three separate type I SLMs that were purchased at different times over the past 2 yr. All three type I SLMs consistently showed similar directional dependence, as shown in Figs. 2(a) to 2(d). In a separate experiment, such a directionality was clearly confirmed for type II SLMs also. The type III SLM showed directionality reproducibly, unless special care was taken in selecting electronic video drivers.



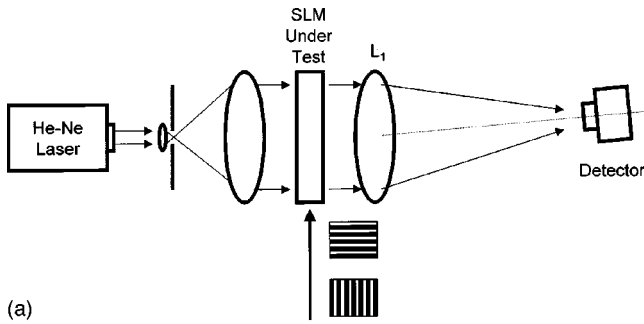
**Fig. 2** Experimental microscopic images of gratings with various orientations and periods: (a) to (d) were obtained with type I and type II LC SLMs and (e) and (f) were obtained with a type III LC SLM.

Figure 3(a) shows an experimental setup for measuring the transfer function of an SLM. An input pattern with various frequencies and orientations is generated by a computer, displayed on the SLM, and Fourier transformed by lens  $L_1$  ( $f = 25$  cm). A detector located at the focal plane detects the intensity of the first-order and zeroth-order diffracted beams. Diffracted efficiency ( $\eta$ ) is defined as the intensity ratio of the first order with respect to the zeroth-order beam.

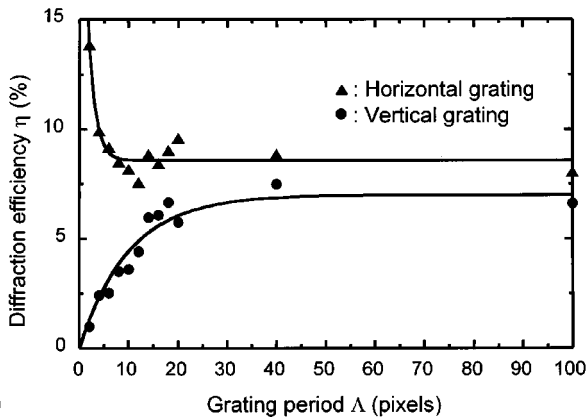
Figure 3(b) shows diffraction efficiency ( $\eta$ ) as a function of grating period ( $\Lambda$  in pixels) for two different grating orientations (horizontal fast-scan and vertical slow-scan directions). As can be seen in the Figure, the horizontal gratings show high response over a broad range of grating periods, even up to the highest frequency of  $\Lambda = 2$  pixels, while vertical gratings have poor efficiency at small grating periods.

#### 4 Application of the Directionality of an SLM to Joint Transform Correlation

The significant difference in the transfer function of an SLM between the horizontal and vertical directions can be efficiently used to improve the performance of a joint transform correlator (JTC). To prove the concept of the idea experimentally a JTC was built, as shown in Fig. 4. Light from a 5 mW He-Ne laser is expanded and the collimated beam is divided into two parts by a beamsplitter: the first part illuminates SLM-1, and the second part illuminates SLM-2. Both the input and reference patterns are located side by side in the input plane on SLM-1. The holographic interference pattern of their Fourier spectra is detected by CCD-1. The NTSC video output from CCD-1 is converted



(a)



(b)

**Fig. 3** (a) Schematic diagram of an experimental setup to measure transfer function of SLMs and (b) transfer function of a type I SLM for horizontal gratings oriented along the fast scan direction (triangles) and vertical gratings along the slow scan direction (circles).

to a VGA signal and is loaded onto SLM-2. The Fourier transform (F.T.) of the hologram recorded on SLM-2 is detected by CCD-2 to obtain the correlation. To measure output over a broad dynamic intensity range, a variable attenuator is located in front of CCD-2.

Figure 5 shows the correlation outputs obtained from the system. To compare correlation performance along the two different directions, three images of the same fingerprints are arranged as shown in Fig. 5(a), each separated by the same distance ( $D=143$  pixels) along both the horizontal and vertical directions. Figure 5(b) shows the correlation

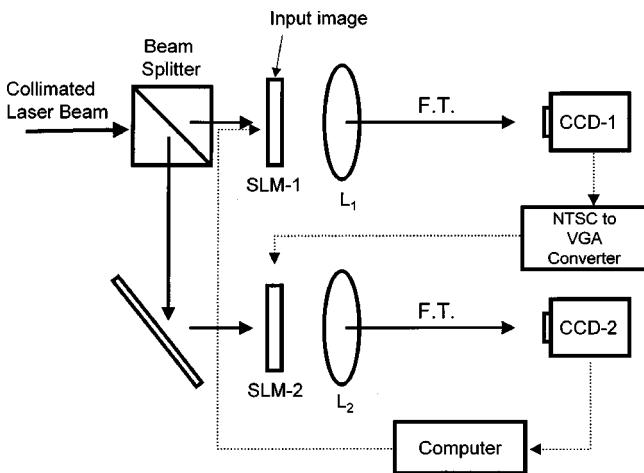


**Fig. 4** JTC setup.

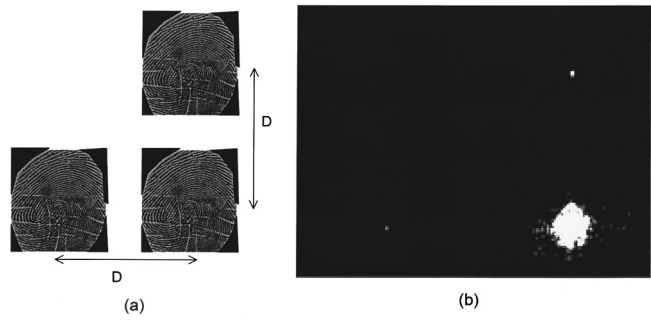


**Fig. 5** (a) Input and (b) correlation output, the autocorrelation signal is much brighter along the vertical direction than along the horizontal direction.

output. As expected, the correlation bright spot is much stronger along the vertical direction than along the horizontal direction. This result clearly demonstrates that our idea of orienting SLM-2 so that the grating runs along the fast horizontal direction works well.

Figure 6 shows the intensity of the autocorrelation peak outputs as a function of grating period of a hologram, which is inversely proportional to the distance ( $D$ ) between an input pattern and a reference pattern in the input plane. As shown in the figure, the orientation of the fast scan direction of an SLM along the grating direction (marked with triangles) renders significantly better performance than that for the orthogonal direction (marked with circles). Note that the discrepancy between these results and those shown in Fig. 3(b) is attributed to the phase nonuniformity of the SLMs and the limited resolution of CCD-1.

### 5 Analysis

The transfer function of an SLM is related to the usable input space-bandwidth product (SBP) of a JTC. Assume that the spatial widths of an input and a target are  $W_1$  and  $W_2$ , respectively, and the two are separated by distance  $D$  in the input plane. As  $D$  increases, the grating period of the interference pattern becomes shorter and eventually becomes limited by the maximum resolution of an SLM-2.

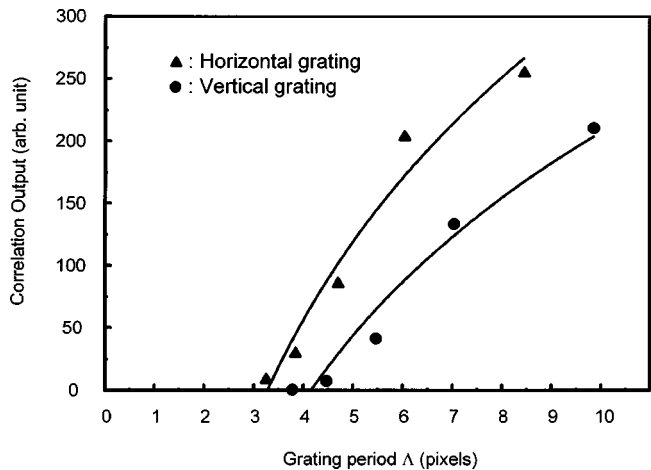


**Fig. 6** Correlation output versus grating period for input and reference patterns arranged along the vertical (triangles) and horizontal (circles) directions.

The maximum allowable distance ( $D_{\max}$ ) between the two inputs is given by  $\lambda f_1 / \Lambda_c$ , where  $\lambda$  is the wavelength of the input beam,  $f_1$  is the focal length of lens  $L_1$ , and  $\Lambda_c$  is the cutoff period or the minimum spatial period of SLM-2. To separate the correlation output from the zeroth-order term, the spatial bandwidths  $W_1$  and  $W_2$  of the two input patterns on liquid crystal TV1 (LCTV1) are limited by the following equation:

$$D_{\min} = \left[ \frac{1}{2} (W_1 + W_2) + \frac{1}{2} (2W_1, 2W_2)_{\max} \right], \quad (1)$$

where  $(2W_1, 2W_2)_{\max}$  is the maximum value of  $2W_1$  and  $2W_2$ . The SBP available for an input is given by

$$\text{SBP} = D_{\max} - D_{\min} + W_2. \quad (2)$$

Assuming that the bandwidths  $W_1$  and  $W_2$  of the two input patterns are same,  $W_1 = W_2 = W$ , SBP becomes

$$\text{SBP} = \frac{\lambda f_1}{\Lambda_c} - W \quad (\text{for } W_1 = W_2 = W). \quad (3)$$

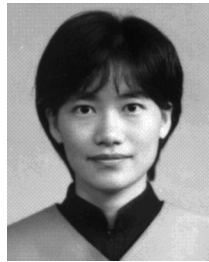
## 6 Conclusion

We quantitatively characterized the differences in the transfer function of an SLM along both fast (horizontal) and slow (vertical) scan directions. Based on this result, we proposed and demonstrated that the performance of a JTC can be significantly improved by arranging the input and reference images along the vertical direction of an SLM so that the holographic grating is oriented along the horizontal (fast scan) direction.

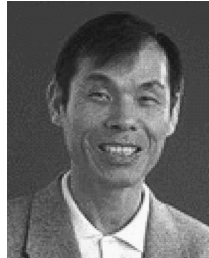
In this simple demonstration, both inputs (an input and a target) are separated vertically, and all the SLMs and CCDs are oriented along the conventional direction—longer dimension along the horizontal direction—to ensure that the holographic grating runs along the horizontal (fast scan) direction of the second SLM. Alternately, the inputs can also be arranged horizontally side by side and CCD-1 can be rotated by 90 deg from the conventional arrangement, so that the grating direction in the second SLM is along the fast scan direction.

## References

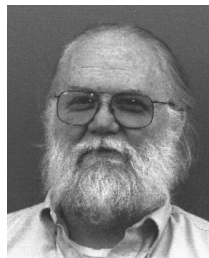
1. C. S. Weaver and J. W. Goodman, "A technique for optically convolving two functions," *Appl. Opt.* **5**(7), 1246–1249 (1966).
2. A. Vanderlugt, "Signal detection by complex spatial filtering," *IEEE Trans. Inf. Theory* **IT-10**, 139–145 (1964).
3. F. T. S. Yu and X. J. Lu, "A real-time programmable joint transform correlator," *Opt. Commun.* **52**, 10–16 (1984).
4. B. Javidi and C. Kuo, "Joint transform image correlation using a binary spatial light modulator at the Fourier plane," *Appl. Opt.* **27**, 663 (1988).
5. P. Tayebati, E. Canoglu, C. Hantzis, and R. Sacks, "High-speed all-semiconductor optically addressed spatial light modulator," *Appl. Phys. Lett.* **71**(12), 1610–1612 (1997).



**Mei-Li Hsieh** received her BS in electro-optical engineering in 1994 and her MS in electro-optical engineering in 1996, both from the National Chiao Tung University in Taiwan. During 1998 she was a guest researcher in the Visual Image Processing Group of Information Access and User Interfaces Division at the National Institute of Standards and Technology. She is currently a PhD candidate in the Institute of Electro-Optical Engineering at the National Chiao Tung University. Her research areas are holographic storage, optical computing, optical spatial light modulator devices, and optical image processing.



**Eung-Gi Paek** received his BSc degree in physics from the Seoul National University in 1972 and his MSc and PhD degrees in physics from the Korea Advanced Institute of Science in 1976 and 1979, respectively. In April 1982, he joined the California Institute of Technology as a postdoctoral fellow and later as a senior research fellow for a period of 5 years. In early 1987, he became a permanent member of technical staff and a principal investigator with the Physical Science and Technology Group of Bellcore (Bell Communications Research in Red Bank, New Jersey). During his 7 year stay at Bellcore, he investigated various applications of photonic devices interacting with device and material scientists. He later joined Rockwell Science Center to contribute to the Defense Advanced Research Projects Agency holographic storage project for a year until he moved to the National Institute of Standards and Technology (NIST) in March 1995. Currently he is a physicist with the Information Technology Laboratory of NIST. He is a fellow of both SPIE and the OSA and he is topical editor of *Optics Letters*.



**Charles L. Wilson** has worked in various areas of computer modeling ranging from semiconductor device simulation, for which he received a Department of Commerce gold medal in 1983, and computer aided design to neural network pattern recognition at Los Alamos National Laboratory, AT&T Bell Laboratories and for the last 19 years the National Institute of Standards and Technology. He currently manages the Visual Image Group in the Information Access and User Interface Division. His current research interests are the application of statistical pattern recognition, neural network methods and dynamic training methods for image recognition, image compression, optical information processing systems and the standards used to evaluate recognition systems.



**Ken Y. Hsu** received his BS in electro-optical engineering in 1973 and his MS in electronic engineering in 1975, both from the National Chiao Tung University in Taiwan, and his PhD in electrical engineering from the California Institute of Technology in 1989. He is currently a professor with the Institute of Electro-Optical Engineering at the National Chiao Tung University. His research interests are optical computing, optical neural networks, optical devices and holography for information processing. He has published more than 70 technical papers in these research fields.